RayWatch: Hemispherical Diffusion on Wrist UV Sensor for Indoor-Outdoor Sensing

Harrison Dong[1,2], Glenn Fernandes[1,2], Christopher Romano[1,2], Yuxin Du[2,3], Tanmeet S. Butani[2], Neel Pendse[2,4], Farzad Shahabi[1,2], Tammy Stump[5], Nabil Alshurafa[1,2]
[1]Department of Computer Science and [2]Department of Preventive Medicine, Northwestern University, Evanston, IL, USA
[3]Department of Computer Engineering, Northwestern University, Evanston, IL, USA
[4]School of Computing, DePaul University, Chicago, IL, USA
[5]Huntsman Cancer Institute, University of Utah, Salt Lake City, UT, USA

***Abstract*—Excessive ultraviolet (UV) exposure is the principal driver of melanoma, yet at-risk individuals seldom receive timely, context-aware cues to apply protection. Existing wrist-worn UV monitors often struggle to recognize timely outdoor exposure because UV readings vary sharply with wrist orientation and sensor angle. To address this gap, we developed a wrist-watch form-factor device that embeds an AS7331 UV photodiode beneath a hemispherical polytetrafluoroethylene (PTFE) dome, which diffuses incident light and stabilizes the sensor's angular response. Ten participants wore the device during routine daily activities, generating more than 93k datapoints of annotated indoor–outdoor data. We implemented an on-device logistic-regression classifier, integrating UVA, UVB, and inertial features to distinguish indoor from outdoor contexts. Under leave-one-participant-out cross-validation, the PTFE-dome watch achieved 94% accuracy and a weighted F1 score of 0.95, outperforming both a flat-window GUVA-S12SD sensor (71% accuracy, F1 = 0.72) and a cylindrical-PTFE enclosure (84% accuracy, F1 = 0.85). By coupling a compact PTFE dome with on-device machine learning (ML), our system delivers reliable, on-wrist UV context sensing and paves the way for unobtrusive, personalized interventions to reduce cumulative UV exposure.**

I. Introduction

Excessive exposure to ultraviolet radiation (UVR) increases the risk of developing melanomas [1]. In response, many wearable devices, often on the wrist, have been developed to track sun exposure in real time [2]. These devices often output an easily digestible UV Index or UV dose value [3] and allow users to understand how much radiation they are exposed to throughout the day. However, more work is needed to connect UV exposure data to evidence-based behavior change techniques such as self-monitoring, feedback, and action planning.

Knowing when an individual is indoors or outdoors is often critical in informing effective UV-related behavior change measures. Moreover, automatic detection of an individual's "indoor-outdoor" state can be very useful in conducting longitudinal analyses of outdoor activity patterns over time, which can guide more effective sun protection planning and behaviors.

This work is supported by the National Cancer Institute, National Institutes of Health with research ID #1R34CA283480-01A1.

While indoor-outdoor detection appears to be a simple problem on its face—UVR is scant indoors and abundant outdoors during daytime hours—most commercially available devices and research prototypes still fall short. First, **optical design:** flat sensor windows accept light over a narrow solid angle, so readings collapse to indoor-like levels whenever the device turns away from the sun or is in shade [4]. Second, **algorithmic oversimplification:** existing pipelines often map raw irradiance directly to exposure dose, ignoring inertial cues that could disambiguate variations in readings due to variations in sensor orientation [5]. These limitations undermine reliable detection of indoor-outdoor state.

To address these gaps, we introduce RayWatch, a wrist-worn UV sensing platform that utilizes on-device ML for robust indoor-outdoor detection. A hemispherical polytetrafluoroethylene (PTFE) dome diffuses incident light [6], broadening angular acceptance and mitigating orientation-induced signal loss. A logistic-regression model then fuses UVA, UVB and inertial (pitch, roll) features to infer indoor-outdoor state. Our ten-participant field study demonstrates that this combined hardware–software approach maintains a clear irradiance differential across natural wrist movement and heterogeneous lighting. In this paper, we present three main contributions:

1) **Optical design:** a hemispherical PTFE dome that enables orientation-robust UV sensing on the wrist.
2) **Machine-learning pipeline:** a lightweight logistic-regression classifier, validated with leave-one-participant-out cross-validation, for real-time indoor-outdoor detection.
3) **Feature analysis:** an empirical evaluation showing how spectral and inertial features jointly drive accurate discrimination among indoor and outdoor conditions.

II. Methods

This section details the wrist-worn system's hardware, the hemispherical PTFE diffuser that stabilizes angular response, the in-the-wild data-collection protocol, and the machine-learning pipeline used to train and evaluate a logistic-regression model for indoor–outdoor detection.

Fig. 1. System overview. (a) Hardware components: electronics assembly, enclosure with hemispherical PTFE dome, and fully assembled wearable. (b) Device worn on the wrist. (c) Example time series of UV measurements with corresponding logistic-regression output classification of indoor and outdoor segments.

A. System Design

We developed a wrist-worn wearable that enables unobtrusive, real-time monitoring of UV exposure and indoor–outdoor context. We measured UV irradiance with an ams AS7331 spectral sensor that outputs readings for UVA, UVB, and UVC (μW cm^{-2}). The sensor interfaced with a Seeed Studio XIAO nRF52840 Sense module with Bluetooth Low Energy (BLE), a 2MB onboard flash, and an LSM6DS3 six-degree-of-freedom inertial measurement unit. We mounted a hemispherical polytetrafluoroethylene (PTFE) dome above the photodiode to diffuse incident light and stabilise the sensor's angular response (Fig. 1a). We enclosed all components in a 3D-printed case compatible with standard watch straps, creating a compact, low-cost platform suitable for everyday use.

The device draws power from a 3.7V, 350 mAh Li-Po battery. We sampled UV data at 4Hz and transmitted it to a smartphone application via BLE whenever a connection was available; otherwise, the firmware buffered the data in the onboard flash for later retrieval. The firmware uses 19360 bytes of RAM—8.1% of the nRF52840's memory capacity. The device draws an average of 4.3mA of current when connected and 7.5mA when disconnected and advertising over BLE, enabling all-day wear with 46.7 hours of continuous operation in the worst case. The device and enclosure weigh a total of 19g, less than the standard smartwatch.

B. Hemispherical Diffusing Sensor Window

Preliminary tests revealed that the AS7331 (UV sensor) alone exhibits a pronounced angular dependence: irradiance readings decrease sharply as the incident angle deviates from normal. Given the high variability of wrist orientation during daily activities, this behavior compromises reliable context (indoor-outdoor) sensing. A common mitigation strategy is to place an optical diffuser over the detector to randomize incident angles and improve the cosine response [7]. We selected PTFE as the diffuser material because it is inexpensive, readily machinable, and provides nearly Lambertian transmission across the UV spectrum [6].

TABLE I
EXAMPLE MINIMUM OUTDOOR AND MAXIMUM INDOOR UVB IN $\mu W/cm^2$ AT DIFFERENT SOLAR AZIMUTH ANGLE DIFFERENCES.

	0°	90°	180°	270°	Indoors
Dome (1mm PTFE Plastic)	4.8	3.51	1.66	4.06	0.92
Flat (0.09mm PTFE Tape)	3.14	0.92	1.1	0.92	0.92

However, experiments with a conventional flat PTFE window showed that with the sensor plane rotated 90° or more away from the solar vector—typical for a wrist-worn device—outdoor irradiance often fell to indoor-like levels (Table I), especially in shaded environments.

To resolve this limitation, we installed a hemispherical window fabricated entirely from PTFE over the UV photodiodes. Hollowed with a wall thickness of 1mm, the dome's near-Lambertian scattering admits UV radiation from a broad solid angle, so outdoor irradiance remains distinctly higher than indoor levels—even in shade or when the wrist faces away from the Sun [8].

C. User Study

We conducted an in-the-wild evaluation to assess the impact of a hemispherical PTFE dome on the accuracy of indoor–outdoor classification. The study protocol was approved by Northwestern University's Institutional Review Board (IRB #STU00224409).

Ten participants (6 urban, 4 suburban) were recruited from the Chicago and Evanston, IL areas. Each participant wore three wrist-mounted UV sensing devices on the same wrist: (1) our custom-built AS7331 spectrometer with a hemispherical PTFE dome, (2) a commercially available GUVA-S12SD UV sensor with a flat diffusing window, and (3) a commercial research grade UV dosimeter developed by Allen et al. [3], which features a cylindrical PTFE enclosure calibrated against a spectroradiometer. This arrangement ensured all devices experienced the same angle of exposure to ambient UV radiation. Participants were instructed to complete 10 transitions between indoor and outdoor environments, with each transition defined

as a single switch from indoors to outdoors or vice versa. The study was designed to reflect natural usage: participants determined the timing and order of their transitions, with the only constraints being a minimum total study duration of 15 minutes and a minimum segment duration of 60 seconds in either context.

While outdoors, participants walked freely in their chosen direction; indoors, they could remain near windows or move farther away, introducing variation in light exposure and wrist motion. Participants used a mobile app to annotate their indoor–outdoor status, providing ground truth labels. Our device recorded separate UVA and UVB values, while the GUVA-S12SD and the Allen device each reported a single UV index value. Data were collected at various times of day to capture changes in solar angle, across multiple weather conditions (sunny, partly cloudy, overcast), and in both shaded and unshaded settings. Recordings were gathered in urban environments (e.g., downtown Chicago) as well as suburban areas (e.g., North Chicago, Evanston) to account for environmental diversity.

TABLE II
STUDY PARAMETERS FOR EACH PARTICIPANT

Participant	Location	Weather	Start
P1	Downtown Chicago	Sunny	1:57pm
P2	Downtown Chicago	Sunny	4:00pm
P3	North Chicago	Sunny	9:05am
P4	Evanston	Cloudy	1:17pm
P5	Evanston	Cloudy	3:22pm
P6	Downtown Chicago	Partly Cloudy	12:56pm
P7	Downtown Chicago	Cloudy	2:43pm
P8	Downtown Chicago	Cloudy	3:30pm
P9	Downtown Chicago	Sunny	12:41pm
P10	Evanston	Partly Cloudy	4:04pm

D. Indoor-Outdoor Detection Model

We used a logistic regression model for indoor–outdoor classification due to its low computational cost and suitability for on-device inference. The model was trained on 93,488 labeled data points collected during our user study. Each point included four features: UVA, UVB, pitch, and roll, and was labeled as -1 (indoor) or +1 (outdoor) using ground truth from a mobile app. To incorporate temporal context, we applied a non-overlapping sliding window approach. Each window was consolidated into a single engineered feature vector containing the min, max, mean, and standard deviation of points in the window (16 total features) and adopting the window's last time point's label. We evaluated a range of window sizes from 10 to 40 samples, corresponding to 2.5–10 seconds for the AS7331 and GUVA-S12SD (sampled at 4 Hz), and 2-40 samples, or 8–320 seconds for the Martin Allen device (sampled at 0.125 Hz). Model performance was assessed using leave-one-participant-out cross-validation. For each device, we computed weighted averages of accuracy, precision, recall, and F1 score across all folds. The best-performing window size for each device was selected based on the highest weighted F1 score.

III. RESULTS

A. Indoor-Outdoor Classification Results

Table III summarizes the weighted average performance across all cross-validation folds, using the best-performing window size for each device. The AS7331 with dome achieved the highest overall accuracy (0.94 ± 0.05), with an F1-score, precision, and recall of 0.95.

In contrast, the GUVA-S12SD achieved significantly lower performance (accuracy: 0.71 ± 0.13, F1-score: 0.72), likely due to its flat window restricting incident light angles. The Martin Allen device performed better than the GUVA-S12SD (accuracy: 0.84 ± 0.10, F1-score: 0.85), but was still outperformed by the AS7331. These results suggest that the hemispherical dome design enables more consistent detection of ambient UV signals under varied conditions.

Per-participant results for the AS7331 device are shown in Table IV. The model maintained high classification performance across all participants, with accuracy and F1-scores ranging from 0.85 to 1.00.

TABLE III
WEIGHTED AVERAGE CLASSIFICATION METRICS ACROSS CROSS-VALIDATION FOLDS PER DEVICE

Sensor	Best Window Size	Accuracy Mean ± StDev	Precision	Recall	F1_score
AS7331 + dome	32	0.94 ± 0.05	0.95	0.95	0.95
GUVA-S12SD	37	0.71 ± 0.13	0.79	0.74	0.72
Martin Allen	3	0.84 ± 0.10	0.88	0.86	0.85

TABLE IV
AS7331 CLASSIFICATION METRICS FOR EACH CROSS-VALIDATION FOLD

Participant	Accuracy	Precision	Recall	F1-score
P1	0.96	0.96	0.96	0.96
P2	0.90	0.90	0.90	0.90
P3	0.98	0.98	0.98	0.98
P4	1.00	1.00	1.00	1.00
P5	0.87	0.89	0.87	0.87
P6	0.92	0.93	0.92	0.92
P7	0.85	0.89	0.85	0.85
P8	0.96	0.96	0.96	0.96
P9	0.96	0.96	0.96	0.96
P10	0.97	0.97	0.97	0.97

B. Visual Data Analysis

To qualitatively assess the separability of indoor and outdoor samples across devices, we applied Principal Component Analysis (PCA) to the windowed feature data corresponding to each device's best-performing window size. As shown in Figure 2, the AS7331 with the hemispherical PTFE dome exhibits a visibly clearer separation between indoor and outdoor samples while the GUVA-S12SD and the Martin Allen device show much more overlap, likely due to their form factors being more sensitive to wrist orientation and line-of-sight to the Sun.

C. Feature Importance

Model explainability analysis using SHAP (Figure 2) reveals that engineered statistical features provide a highly

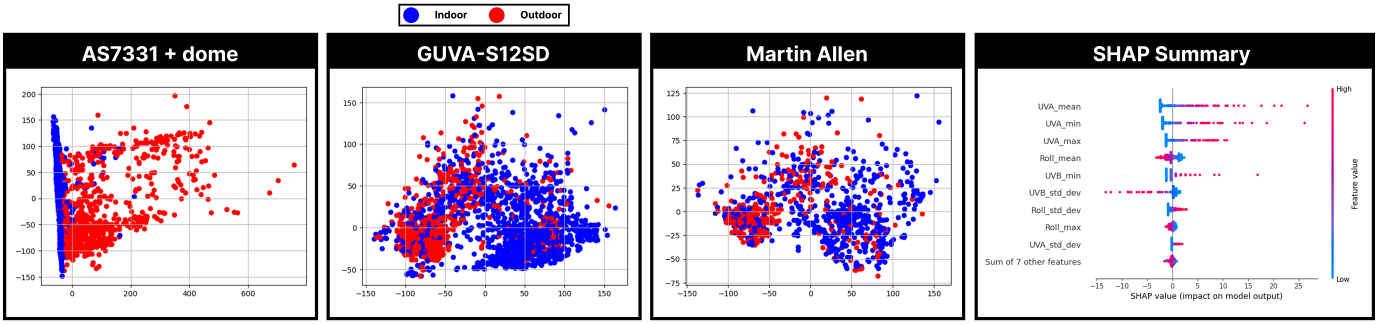

Fig. 2. (From Left) Samples for each device mapped to 2 dimensions using PCA (dimensionless), SHAP plot for features in indoor-outdoor prediction.

interpretable framework for classification. The model identifies the mean UVA radiation (UVA_mean) as the most salient predictor, where its value demonstrates a strong bipolar influence, pushing predictions toward "Outdoor" when high and "Indoor" when low. The model also leverages more subtle cues from motion sensors. Device orientation, specifically a higher Roll_mean, correlates negatively with the "Outdoor" class. As expected, Roll_std_dev illustrates that low device stability and more movement (high standard deviation) is typically associated with outdoor environments, with the model correctly assigning it a positive contribution towards an "Outdoor" classification.

IV. Discussion

To assess classification performance near state transitions, we analyzed samples centered around "transition points"—moments when participants moved from indoor to outdoor environments or vice versa. For each device, the best-performing window size was centered on these transitions, resulting in mixed indoor and outdoor data, and labeled according to the latter state (i.e., the label reflects the new environment).

As shown in Table V, classification accuracy at these transition points is substantially lower for the AS7331 with dome and the Martin Allen device. This highlights a key limitation: real-time detection of environment changes remains challenging, even with our hardware improvements. While more powerful or temporally-aware models (e.g., recurrent architectures) may improve accuracy during such transitions, they may also introduce computational and energy costs that are undesirable for on-device inference.

TABLE V
Classification Accuracy At and After Transitions

Sensor	Transition Accuracy	Post-Transition Accuracy
AS7331 + dome	0.77	1.00
GUVA-S12SD	0.74	0.89
Martin Allen	0.78	0.89

Encouragingly, performance improves markedly in the windows immediately after a transition, especially for our device, shown under "Post-Transition Accuracy" in Table V. This suggests that our system can reliably detect indoor–outdoor changes within approximately 12 seconds of a transition when using 32-point windows. Future work could explore hybrid model architectures or adaptive windowing strategies to reduce this latency while maintaining energy efficiency.

V. Conclusion

We presented a wrist-worn UV sensing system that combines a compact hemispherical PTFE dome with the AS7331 spectral UV sensor to improve on-body detection of indoor and outdoor contexts. In a real-world study with ten participants, our device outperformed two common UV monitor designs—a flat-window GUVA-S12SD and a commercial research grade cylindrical-PTFE enclosure—in classification accuracy and F1 score. The on-device logistic regression model, which integrates UVA, UVB, and inertial features, achieved reliable predictions within 12 seconds of transition events, despite challenges with mixed indoor–outdoor segments. By stabilizing angle-dependent readings through the dome design and enabling lightweight, on-wrist inference, our system offers a practical pathway toward real-time, context-aware sun exposure tracking and intervention.

References

[1] J. Lopes, C. M. Rodrigues, M. M. Gaspar, and C. P. Reis, "Melanoma management: from epidemiology to treatment and latest advances," *Cancers*, vol. 14, no. 19, p. 4652, 2022.

[2] C. Lin, Y. Du, N. Pendse, G. Fernandes, N. Alshurafa, and M. Pedram, "Self-sustaining wearable uv sensor for passive and continuous sun protection," in *2024 IEEE 20th International Conference on Body Sensor Networks (BSN)*. IEEE, 2024, pp. 1–4.

[3] M. W. Allen, N. Swift, K. M. Nield, B. Liley, and R. L. McKenzie, "Use of electronic uv dosimeters in measuring personal uv exposures and public health education," *Atmosphere*, vol. 11, no. 7, p. 744, 2020.

[4] P. Weihs, A. Schmalwieser, C. Reinisch, E. Meraner, S. Walisch, and M. Harald, "Measurements of personal uv exposure on different parts of the body during various activities," *Photochemistry and photobiology*, vol. 89, no. 4, pp. 1004–1007, 2013.

[5] A. Henning, N. J. Downs, and J. K. Vanos, "Wearable ultraviolet radiation sensors for research and personal use," *International journal of biometeorology*, vol. 66, no. 3, pp. 627–640, 2022.

[6] V. R. Weidner and J. Hsia, "Reflection properties of pressed polytetrafluoroethylene powder," *Journal of the Optical Society of America*, vol. 71, pp. 856–861, 1981.

[7] G. Seckmeyer and G. Bernhard, "Cosine error correction of spectral uv-irradiances," in *Atmospheric Radiation*, vol. 2049. SPIE, 1993, pp. 140–151.

[8] F. Ott and A. Kienle, "Lambertian illumination of dielectric scattering media with monochromatic light," *Physical Review A*, 2022.